Available online at www.sciencedirect.com
ScienceDirect
Journal of Hazardous Materials 153 (2008) 478–486
Journal of Hazardous Materials
www.elsevier.com/locate/jhazmat

Competition of Reactive red 4, Reactive orange 16 and Basic blue 3 during biosorption of Reactive blue 4 by polysulfone-immobilized *Corynebacterium glutamicum*

K. Vijayaraghavan *, Yeoung-Sang Yun *

Division of Environmental and Chemical Engineering, Research Institute of Industrial Technology, Chonbuk National University, Chonju 561-756, South Korea

Received 3 June 2007; received in revised form 28 August 2007; accepted 28 August 2007
Available online 1 September 2007

Abstract

Competition of Reactive red 4 (RR4), Reactive orange 16 (RO16) and Basic blue 3 (BB3) during biosorption of Reactive blue 4 (RB4) by polysulfone-immobilized protonated *Corynebacterium glutamicum* (PIPC) was investigated in batch and column mode of operations. Through potentiometric titrations, and with the aid of proton-binding model, carboxyl, phosphonate and amine were identified as functional groups of PIPC, with apparent pK_a values of 3.47 ± 0.05, 7.08 ± 0.07 and 9.90 ± 0.05 mmol/g, respectively. Since reactive dyes release dye anions ($ROSO_3^-$) in solutions, the positively charged amine groups were responsible for biosorption. PIPC favored biosorption at pH 3 when RB4 was studied/used as single-solute; while the presence of RR4 and RO16 severely affected the RB4 biosorption. When present as a single-solute, PIPC recorded 184.5 mg RB4/g; while PIPC exhibited 126.9, 120.9 and 169.6 mg RB4/g in the presence of RR4, RO16 and BB3, respectively. In general, the accessibility of amine group depends on the molecular size, number of sulfonate groups and reactivity of each reactive dye. Single and multicomponent Freundlich equations successfully described the biosorption isotherms. With 0.1 M NaOH, it is possible to reuse PIPC for RB4 biosorption in 10 repeated cycles. Column experiments in an up-flow packed column coincided with batch results, that is PIPC showed strong preference towards highly reactive and relatively small RB4 anions; however, the presence of competing dyes hinder the RB4 column biosorption performance.

Keywords: Multicomponent; Isotherm; Kinetics; Immobilization; Packed column

1. Introduction

In recent years, fermentation wastes are portrayed as potential sorbents for dye molecules [1,2]. One such waste is *Corynebacterium glutamicum*, generated in lysine fermentation industries. *C. glutamicum*, a Gram-positive organism, belonging to the order of Actinomycetales, is widely used for the biotechnological production of amino acids. Currently, the production of amino acids in fermentation processes with *C. glutamicum* amounts to 1,500,000 t of L-glutamate and 550,000 t of L-lysine per year [3]. Hence, the wastes generated after the process are high; however, they are not often recycled as animal feed or as organic manure but are incinerated or dumped at sea [1].

Our previous studies identified *C. glutamicum* as an excellent biosorbent for reactive dyes [4–6]. However, the free biomass posed problems when biosorbent reuse was attempted. It is well known that microorganisms such as bacteria and fungi have poor mechanical strength and little rigidity [5,7]. These factors limit their application in real conditions despite their high dye binding abilities. Immobilization is the possible and practical method for successful reuse of biosorbent in multiple cycles. The choice of immobilization matrix is a key factor in environmental application of immobilized biomass and it determines the mechanical strength and chemical resistance of the final biosorbent particle [8].

Although most industrial effluents contain several dye components; little attention has been given to multicomponent adsorption systems [9]. Many problems are to be solved for multicomponent biosorption, the important being the evaluation of competition between solutes in occupying the limited binding sites. Multicomponent dye adsorption has been the subject of

* Corresponding authors. Tel.: +82 63 270 2308; fax: +82 63 270 2306.
E-mail addresses: drkvijy@chonbuk.ac.kr (K. Vijayaraghavan), ysyun@chonbuk.ac.kr (Y.-S. Yun).

0304-3894/$ – see front matter © 2007 Elsevier B.V. All rights reserved.
doi:10.1016/j.jhazmat.2007.08.079

Nomenclature

b	Langmuir equilibrium constant (L/mg)
b_j	moles of functional group per gram of biomass (mmol/g)
BB3	Basic blue 3
C_1	equilibrium or final concentration of component 1 (mg/L)
C_2	equilibrium or final concentration of component 2 (mg/L)
C_A	concentration of component A
C_B	concentration of component B
C_f	equilibrium or final dye concentration (mg/L)
d_1	optical density or absorbance at λ_1
d_2	optical density or absorbance at λ_2
dc/dt	slope of the breakthrough curve from breakthrough to exhaustion time (mg/(L h))
k_i	intraparticle diffusion constant (mg/(g min$^{0.5}$))
K_{A1}	calibration constant for component A at wavelength λ_1
K_{A2}	calibration constant for component A at wavelength λ_2
K_{B1}	calibration constant for component B at wavelength λ_1
K_{B2}	calibration constant for component B at wavelength λ_2
K_F	Freundlich constant ((mg/g)(L/mg)$^{-1/n}$)
K_j	equilibrium constant (mol/L)
M	biosorbent mass (g)
n	Freundlich model exponent
N	number of data points
p	number of parameters
PIPC	polysulfone-immobilized protonated *Corynebacterium glutamicum*
q_{eq}	equilibrium dye uptake (mg/g)
$q_{eq,cal}$	calculated equilibrium dye uptake (mg/g)
$q_{eq,meas}$	measured equilibrium dye uptake (mg/g)
$(q_{eq})_i^j$	amount of solute (i) sorbed per unit weight in the presence of solute, j (mg/g)
q_{max}	maximum monolayer coverage capacity of the biosorbent (mg/g)
q_t	uptake at any time (mg/g)
Q	column uptake capacity (mg/g)
R^2	correlation coefficient
RB4	Reactive blue 4
RO16	Reactive orange 16
RR4	Reactive red 4
t	time (h)
t_b	breakthrough time (h)
t_e	exhaustion time (h)
X	biomass dosage (g/L)

Greek symbols

β	selectivity factor
ε	average error (%)
η_1	interaction factor for first dye
η_2	interaction factor for second dye
θ_{ij}	competitive coefficient
λ_1	wavelength at which maximum absorbance of component A obtained (nm)
λ_2	wavelength at which maximum absorbance of component B obtained (nm)

few studies [10,11]; however, the mechanism and competition effect has hardly been understood. The evaluation and predication of multicomponent sorption equilibrium are tedious and they are still most challenging problems in adsorption field.

As studies on multi-dye biosorption in batch mode are relatively limited in number [9], the behavior of multi-dye in column biosorption has not even been attempted. In columns, treating multi-dye mixtures may result in irregular concentration profile and overshoot of particular toxicant; this is because of dye molecules competition over the biosorbent.

Motivated by all these aspects, this study employed polysulfone-immobilized protonated *C. glutamicum* biomass for the biosorption of Reactive blue 4. Multicomponent biosorption has been attempted by selecting three possible binary mixtures (RB4 + RR4, RB4 + RO16 and RB4 + BB3). In addition, the interference of other reactive dyes and basic dye on RB4 biosorption in an up-flow packed column was also attempted.

2. Experimental

2.1. Preparation of biosorbent

The fermentation wastes (*C. glutamicum* biomass) were obtained in the form of dried powder from a lysine fermentation industry (BASF-Korea, Kunsan, Korea). The biomass were grounded and sieved to obtain particle sizes in the range of 0.1–0.25 mm. The biomass (10 g/L) was then protonated with 0.1 M HNO_3 for 1 h at constant temperature (25 °C). After this pretreatment, the biomass was washed with deionized water, and dried in an oven at 60 °C for 12 h.

A 9% (w/v) solution of polysulfone was prepared in *N*,*N*-dimethyl formamide (DMF) solution. After stirring the above mixture for 10 h, the protonated biomass (14%) were mixed with the polysulfone slurry and the resulted slurry was dripped in deionized water, where beads were formed by phase inversion process. Beads were then washed with deionized water, put into a water bath for 18 h in order to remove all residual DMF. The resultant polysulfone-immobilized protonated *C. glutamicum* (PIPC) beads (1–3 mm diameter) were then stored at 4 °C.

2.2. Dyes and analysis

All dyes, used in this study, were purchased from Sigma–Aldrich Korea Ltd. (Yongin, Korea). Dye concentrations were analyzed using a spectrophotometer (UV-2450, Shimadzu,

Kyoto, Japan). For single-dye solutions, the dye concentrations were determined by measuring the optical densities at 595, 517, 494 and 654 nm for RB4, RR4, RO16 and BB3, respectively. Calibration for cross interference was carried out as follows [12]. For a bisolute system of components A and B measured at λ_1 and λ_2, respectively, to give optical densities of d_1 and d_2:

$$C_A = \frac{K_{B_2} d_1 - K_{B_1} d_2}{K_{A_1} K_{B_2} - K_{A_2} K_{B_1}} \quad (1)$$

$$C_B = \frac{K_{A_1} d_2 - K_{A_2} d_1}{K_{A_1} K_{B_2} - K_{A_2} K_{B_1}} \quad (2)$$

where C_A and C_B are the concentrations of components A and B, respectively; K_{A_1}, K_{B_1}, K_{A_2} and K_{B_2} are the calibration constants for components A and B at the two wavelengths λ_1 and λ_2, respectively. The standard calibration curves were linear for each dye with correlation coefficients greater than 0.997.

2.3. Batch experimental procedure

Wet PIPC beads (1 g) were contacted with 40 mL of desired dye concentrations in a 50 mL plastic bottle (high-density polyethylene). For multi-dye solutions, the concentration ratios were always maintained at 1:1 (w/w). The pH of the solution was initially adjusted using 0.1 M HCl or NaOH; and the pH was also controlled using same chemical agents during biosorption experiments. After 16 h of contact, the supernatant was separated and analyzed for dye concentrations, after appropriate dilution. For isotherm experiments, the dye concentrations were in the range of 0–1500 mg/L. In the present study, the uptake capacity of PIPC was reported on the basis of mg of dye biosorbed per gram of dry beads. However, for the sake of better understanding the amount of biomass per gram of dry beads was calculated and based on the mass balance it was determined as 0.56 g biomass/g dry beads.

For desorption experiments, dye-laden PIPC beads (previously exposed to 250 mg RB4/L at pH 3) were contacted with 20 mL of 0.1 M NaOH for 2 h on a rotary shaker at 160 rpm. The remaining procedure was the same as that employed in the biosorption equilibrium experiments.

2.4. Isotherm data modeling

The single-component biosorption isotherms were described using the Langmuir and Freundlich models, which can be expressed in their non-linear forms, as follows:

- Langmuir model:

$$q_{eq} = \frac{q_{max} b C_f}{1 + b C_f} \quad (3)$$

- Freundlich model:

$$q_{eq} = K_F C_f^{1/n} \quad (4)$$

where q_{eq} is the equilibrium dye uptake (mg/g), q_{max} the maximum monolayer coverage capacity of the biosorbent (mg/g), C_f the equilibrium dye concentration (mg/L), b the Langmuir equilibrium constant (L/mg), K_F the Freundlich constant (mg/g)(L/mg)$^{-1/n}$ and n is the Freundlich model exponent.

The multicomponent biosorption isotherms were described using an extended Langmuir equation, with a constant interaction factor [13], which can be represented for binary mixtures, as follows:

$$q_{eq1} = \frac{q_{max1} b_1 (C_1/\eta_1)}{1 + b_1(C_1/\eta_1) + b_2(C_2/\eta_2)} \quad (5)$$

$$q_{eq2} = \frac{q_{max2} b_2 (C_2/\eta_2)}{1 + b_1(C_1/\eta_1) + b_2(C_2/\eta_2)} \quad (6)$$

where q_{max1}, q_{max2}, b_1 and b_2 are the single component Langmuir parameters for the first and second dye, respectively. η_1 and η_2 are the interaction factors for first and second dye, respectively. The calculation of the interaction factor is based on minimizing the following error function [10]:

$$\frac{100}{N-p} \sum_{i=1}^{n} \left[\frac{(q_{eq,meas} - q_{eq,cal})^2}{q_{eq,meas}} \right]_i \quad (7)$$

where N and p are the number of data points and parameters, respectively.

Also, the Sheindrof–Rebhun–Sheintuch (SRS) equation [14] was employed in the present study, which can be represented for binary mixtures as follows [15]:

$$(q_{eq})_i^j = K_{F_i} C_{f_i} [C_{f_i} + \theta_{ij} C_{f_j}]^{[(1/n_i)-1]} \quad (8)$$

where $(q_{eq})_i^j$ is the amount of solute, i, sorbed per unit weight of PIPC in the presence of solute, j, K_{F_i} the single-component Freundlich constant for solute i, n_i the Freundlich exponent for solute i and θ_{ij} is the competitive coefficient. All model parameters were evaluated using non-linear regression employing the Sigma Plot (version 4.0, SPSS, USA) software. The average percentage error between the experimental and predicted values was calculated using:

$$\varepsilon\,(\%) = \sum_{i=1}^{N} \frac{(q_{eq,meas} - q_{eq,cal})/q_{eq,meas}}{N} \times 100 \quad (9)$$

2.5. Potentiometric titration

Titration of biosorbent was carried out at constant temperature (25 °C) using 50 mL plastic bottles (high-density polyethylene) comprising 20 mL CO_2 stripped water and 0.2 g (wet weight) PIPC. In order to obtain different initial pH values in the range of 2–12, a certain amount of 0.1 M HCl or NaOH was added to each of the biomass suspensions. The air-tightened bottles were then agitated at 160 rpm and allowed to equilibrate for 24 h. Thereafter, the equilibrium pH was measured using an electrode (Ingold).

2.6. Column experimental procedure

A glass column (1 cm I.D. and 12 cm height) packed with 4.8 g (wet weight) of PIPC was used to perform continuous

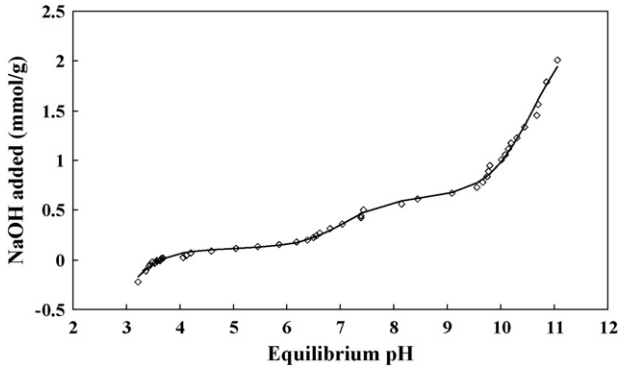

Fig. 1. Potentiometric titration data of PIPC. Curve is predicted by the proton-binding model.

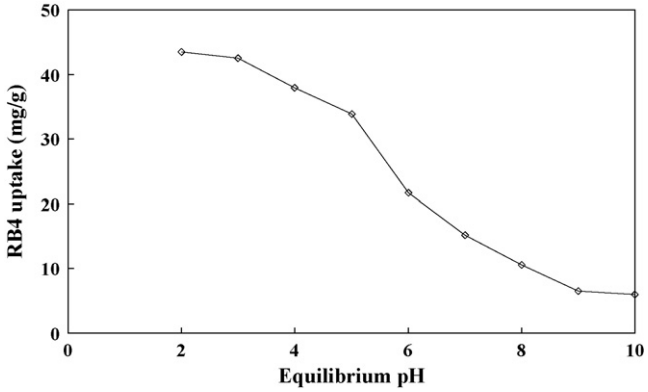

Fig. 2. The effect of equilibrium pH on the RB4 uptake capacity of PIPC (initial dye concentration = 247 mg/L; temperature = 25 °C; agitation rate = 160 rpm).

biosorption experiments. A peristaltic pump was used to pump the dye solution upwards through the column at 0.5 mL/min. Effluent samples were collected at the exit of the column at different time intervals (1–2 h) and analyzed for dye concentration. All column studies were conducted at constant initial solution pH of 3 and at room temperature of 25 ± 1 °C. Column breakthrough and exhaustion times were fixed as the times at which effluent concentration reach 1 and 95% of influent concentration, respectively. The total quantity of dye mass biosorbed in the column is calculated from the area above the breakthrough curve (outlet dye concentration vs. time) multiplied by the flow rate. Dividing the dye mass by the biosorbent mass (M) leads to the uptake capacity (Q) of the biomass.

Regeneration experiments were conducted by employing 0.1 M NaOH as the elutant. The elutant was fed at 1 mL/min and the effluent was analyzed for dye concentration. All the experiments were carried out in duplicates, and the deviations were within 5%.

3. Results and discussion

3.1. Biosorbent characterization

Our past research revealed that free biomass of *C. glutamicum* possesses excellent reactive dye binding capacity [5,6]. However, its application in column operations is a cause of concern, due to its poor mechanical stability, high swelling and solid–liquid separation problems. Therefore in this research, *C. glutamicum* was immobilized in a polysulfone matrix and subsequently employed for biosorption studies.

The PIPC titration data is reported in Fig. 1. These data permit the qualitative and quantitative determination of the nature and number of binding sites present on the PIPC. The curve shows at least three inflexion points in the pH ranges of 3–4, 6.5–7.5 and 9.5–10.5. To describe the titration curve, a proton-binding model as proposed by Yun et al. [16] was used in this study. The final form of the model equation can be expressed as:

$$[\mathrm{Na}]_{\mathrm{added}} = \sum_{j=1}^{N} \left[\frac{b_j X}{1 + ([\mathrm{H}^+]/K_j)} \right] + \frac{K_{\mathrm{W}}}{[\mathrm{H}^+]} - [\mathrm{H}^+] \qquad (10)$$

Eq. (10) contains two parameters per functional group: moles of functional group per gram of biomass (b_j) and the equilibrium constant (K_j). The model assumes the presence of three binding sites. Detailed derivation of the proton-binding model can be found elsewhere [4,16]. To find the number and nature of binding sites, the model was fitted to the titration curve (Fig. 1) using the Marquardt–Levenberg non-linear regression algorithm in Sigma Plot (version 4.0, SPSS, USA) software. Two negative ($\mathrm{p}K_{\mathrm{H}} = 3.47 \pm 0.05$ and 7.08 ± 0.07) and one positive ($\mathrm{p}K_{\mathrm{H}} = 9.90 \pm 0.05$) functional groups were predicted by the proton-binding model. The first site ($\mathrm{p}K_{\mathrm{H}} = 3.47 \pm 0.05$) can be established as carboxyl groups, that have $\mathrm{p}K_{\mathrm{H}}$ values ranging from 3.4 to 5 [16,17]. The number of carboxyl groups was found to be more abundant as 0.84 ± 0.03 mmol/g was predicted by proton-binding model. The second group, whose $\mathrm{p}K_{\mathrm{H}}$ and b_j values were 7.08 ± 0.07 and 0.23 ± 0.01 mmol/g, respectively, can be assigned as phosphonate groups (B-HPO_4^-) or dicarboxylic groups [4]. The last functional group ($\mathrm{p}K_{\mathrm{H}} = 9.90 \pm 0.05$) seemed to be amine groups (B-NH_3^+) that generally shows $\mathrm{p}K_{\mathrm{H}}$ values between 8.5 and 10 depending on the biomaterial [4,18]. Also, the amine groups were found to be second abundant in PIPC ($b_j = 0.79 \pm 0.03$ mmol/g).

3.2. pH edge and isotherm experiments

Between pH 2 and 3, the biosorption of RB4 was found maximum, with removal efficiencies above 94% (Fig. 2). Increasing the pH further decreases the dye uptake. The cell wall of *C. glutamicum* belongs to a distinct and well-separated group within the Gram positives characterized by a unique cell wall organization and possession of unique cell wall components not present in the other Gram positives [19]. In addition to a thick peptidoglycan layer, a second surface layer consists of covalently bound mycolic acids and extractable lipids [20]. Ester bonds link the mycolic acids to the arabinogalactan, which covalently attached to the murein of the cell wall. Potentiometric titrations revealed the presence of carboxyl, phosphonate and amine groups. In acidic pH values, due to protonation of functional groups, the biomass will have net positive charge [4]. On the other hand, reactive dyes release colored negatively charged dye ions in solution, which will exhibit electrostatic attraction towards the

positively charged cell surface. In particular, the amino groups present in *C. glutamicum* were mainly responsible for reactive dye biosorption and the hydrogen ion acts as a bridging ligand between the bacterial cell wall and the dye molecule [6]. Potentiometric titrations revealed that pK_a values of amine group lies around 9.90 ± 0.05, which means amine groups will be completely protonated at a pH less than approximately 7 [2]. In contrast, pH edge experiments indicated that little biosorption occurred at pH > 6. This may be due to the presence of other functional groups such as carboxyl, which are negatively charged and exhibit repulsion towards negatively charged dye anion. Control experiments were also conduced with biomass free polysulfone beads for RB4 biosorption, in which they exhibited 9.8 mg/g dry beads at pH 3.

Fig. 3a shows the representation of the RB4 sorption isotherm, the capacity (Q) of PIPC (in mg/g) against the equilibrium concentration (C_f) at pH 3. The uptake of RB4 increased with increasing dye concentration and reached saturation at higher equilibrium concentration. The Langmuir and Freundlich models were used to represent the RB4 biosorption isotherm; and the model constants are depicted in Table 1. On the basis of correlation coefficients, Freundlich model better described the RB4 isotherm.

3.3. Competitive biosorption and modeling

Three binary dye mixtures (RB4 + RR4, RB4 + RO16 and RB4 + BB3) were used to study the influence of competing dye on RB4 biosorption onto PIPC. Before evaluating the multi-dye systems, the single dye isotherms for all dyes were experimentally determined at pH 3 (Fig. 3a). In general, PIPC performed well in the case of reactive dye biosorption at pH 3. On close comparison, in addition to higher uptake, PIPC exhibited steeper isotherms for RB4 compared to other dyes. However, its performance on BB3 was below par. As we already stated, reactive dye release dye anions, which will attract towards positive cell surface. In contrast, BB3 exist as Dye^+Cl^- in solutions. This means negatively charged biomass surface will favor basic dye biosorption. In particular, carboxyl group will be responsible for basic dye biosorption, as increase in pH transform –COOH into carboxylate anion ($–COO^-$). However, in this study, isotherm experiments were conducted only at pH 3 and under this condition all functional groups will be completely protonated resulting in overall positive charge of the biomass.

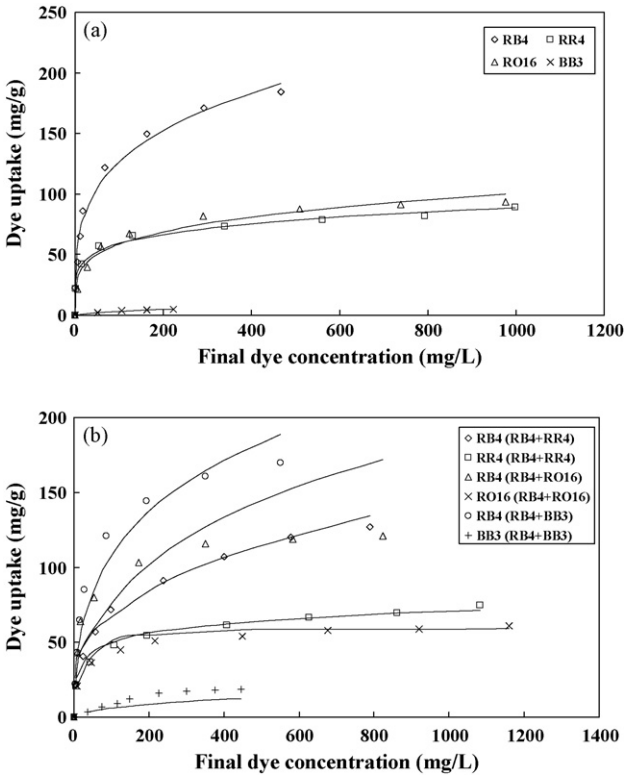

Fig. 3. Single (a) and binary (b) isotherms obtained at pH 3 during dye biosorption onto PIPC. Single-dye isotherm curves were predicted by the Freundlich model and binary dye isotherm curves were predicted by the SRS equation.

Fig. 3b shows the experimental binary-dye biosorption isotherms at pH 3. In the presence of RR4 and RO16, RB4 uptake was severely affected. On the basis of highest dye uptake, the decrease was 31.2 and 34.4% (when comparing the single RB4 isotherm data) in the presence of RR4 and RO16, respectively. The presence of RB4 also affected RR4 and

Table 1
Single and binary dye biosorption isotherm model parameters

Single system	Langmuir model				Freundlich model			
	q_{max} (mg/g)	b (L/mg)	R^2	ε (%)	K_F ((mg/g)(L/mg)$^{-1/n}$)	n	R^2	ε (%)
RB4	180.0	0.048	0.97	3.9	37.0	3.74	0.99	0.1
RR4	85.5	0.052	0.92	6.3	26.1	5.65	0.99	2.3
RO16	94.4	0.026	0.97	4.6	20.2	4.31	0.97	4.3
BB3	7.9	0.007	0.98	1.0	0.26	1.83	0.99	1.1

Binary system	Multicomponent Langmuir model						SRS equation					
	η_1	η_2	R_1^2	R_2^2	ε_1 (%)	ε_2 (%)	θ_{12}	θ_{21}	R_1^2	R_2^2	ε_1 (%)	ε_2 (%)
RB4(1) + RR4(2)	4.0	16.0	0.94	nc	6.9	71.9	0.45	0.71	0.97	0.99	4.4	1.6
RB4(1) + RO16(2)	2.5	5.2	nc	0.89	63.4	7.3	0.30	1.52	0.77	0.91	16.2	5.8
RB4(1) + BB3(2)	1.4	10.9	0.95	nc	4.6	97.4	0.10	0.21	0.89	0.62	3.6	21.6

nc, data not converged.

RO16 uptakes, as 16.4 and 35.1% decrease, respectively, were observed while comparing their respective single-component isotherm data. On contrary, the presence of BB3 not significantly affected RB4 biosorption onto PIPC. Adsorption is a process in which several parameters can be involved, either related to sorbent characteristics (specific surface area, pore size distribution, etc.) or to sorbate structural features (molecular weight, shape, molar volume, flexibility, branching, etc.) [21]. In several instances, adsorption seems to be correlated with the molecular size of dyes: a tendency may be that the smaller the dye is, the more and faster it is sorbed [11,21]. However, it should be noted that, when pores are large enough to admit one dye molecule but too small to admit another one, then pore blockage may be the dominant competition mechanism. However, single component isotherm data revealed that PIPC showed good biosorption capacity towards all three reactive dyes. Therefore direct sites competition may be the predominant competition mechanism [22], with all reactive dyes competing with each other in occupying the same amine group.

The reactive dyes, RR4, RB4 and RO16 are tetra-, di- and mono-sulfonated species. The sulfonate groups are related to reactive dye biosorption and each of them associate with one amine group of PIPC. This accounts for four amine group utilization of RR4, two in the case of RB4 and one amine group for RO16 [11,23] The number of amine groups (0.79 ± 0.03 mmol/g), as calculated from potentiometric titration, can be correlated with uptake capacity (in mmol/g) of PIPC, in respect to each of the examined dye. Taking into consideration the single dye isotherm data, the experimental highest dye uptakes were always lower than the available amine groups. For instance, when assuming two-to-one stoichiometric relationship between amine groups required and RB4 sorbed, there was 1.4 times more amine groups available compared to amines actually involved in binding. This difference was approximately 2.1 and 5.2 times for RR4 and RO16, respectively. The result clearly implied that not all amine groups participated in dye binding; and the extent of binding strongly depends on the type of dye and its solution chemistry. The same phenomenon, i.e., underutilization of amine groups was also observed in the cases of binary systems. However, it is interesting to note that more amine groups participated during binary systems compared to single dye systems. For instance, total molar uptake in RB4–RR4 system was 0.28 mmol/g (0.20 mmol RB4/g and 0.08 mmol RR4/g); and this require 0.72 mmol/g of amine group. Thus the amount of amine group involved during binary biosorption was comparatively higher. The reason for this trend was unclear and has not been reported so far to the authors' knowledge; but probably due to uneven size of the dye molecules and the increasing concentration gradient that forces the adsorption of dyes onto inaccessible amine groups (*Note*: for binary systems total initial dye concentration was 3000 mg/L compared to 1500 mg/L in single systems).

Competitive biosorption data clearly revealed that PIPC exhibited preference towards RB4 compared to other dyes examined. In order to quantify the competitive effect, the selectivity factor (β) of dyes was used and can be defined by [24]:

$$\beta_{1/2} = \frac{q_{eq1}/q_{eq2}}{C_{1,0}/C_{2,0}} \quad (11)$$

where subscripts "1" and "2" represents first and second dye, respectively; q_{eq} and C_0 represents dye uptake and initial dye concentration, respectively.

Clearly, β for RB4/RR4, RB4/RO16 and RB4/BB3 systems increases with increasing their corresponding initial concentrations. This indicates the influence of RB4 towards the amine groups of PIPC. The selectivity factors were observed maximum for RB4/BB3 systems in the range of 4.2–6.0 compared to 1.0–1.7 and 1.0–2.0 for RB4/RR4 and RB4/RO16, respectively. This result supports the fact that at low dye concentrations there were adequate binding sites available to accommodate both dye anions. However, as the concentration increases RB4 competed well and occupied more binding sites. The reason for high RB4 uptakes in all three binary systems may be due to the number of amine groups required for biosorption. This case may be true, when we take RR4 into account; however, as we discussed earlier RO16 require only one amine group compared to two amine groups for RB4. The reactive dyes, RB4, RO16 and RR4 come under Procion, Remazol and Cibacron classes, respectively. According to Fowler and Marshall [25], we can classify Procion class as highly reactive, Remazol as moderately reactive whereas Cibacron is least reactive. Our results based on the molar uptake, clearly coincides with this classification. Reactivity is an important factor during dyeing process that governs the rate of diffusion of dye into the fibre. High reactivity dyes are always favorable as it require less time for batching process; however, it should be noted that reactivity depends on pH and whose enhancement usually increases the dye reactivity [25]. At pH 3, RB4 is highly reactive; whereas strong alkaline conditions are required for RO16 and RR4.

For multicomponent isotherm modeling, an extended Langmuir equation, with a constant interaction factor, was used. The traditional extended Langmuir equation assumes no interaction between solutes; which is not valid in real conditions [10]. To incorporate sorbate–sorbate interactions and competitions, an interaction factor (η) has been introduced into the extended Langmuir equation [13]. In the present study, η was assumed to be constant and specific for each dye in the binary systems, and the values are listed in Table 1. However, the model, in most cases, was unable to describe binary isotherms resulting in poor correlation coefficients and very high % error values. The reason for this discrepancy may be due to competition and interaction between the dye solutes, which was very significant; and the saturation capacity of each dye in single-solute systems was also different [10]. It should be noted that single component Langmuir isotherm model constants were used to model the multicomponent biosorption data, as described in Section 2.4. Also, the interaction factor, η, does not have a strong theoretical foundation, with several investigators having employed the model with only limited success [10,13].

Next the SRS equation, which is a multicomponent Freundlich type equation, was used to describe the binary isotherm data. The model comprised of a competitive coefficient (θ_{ij}),

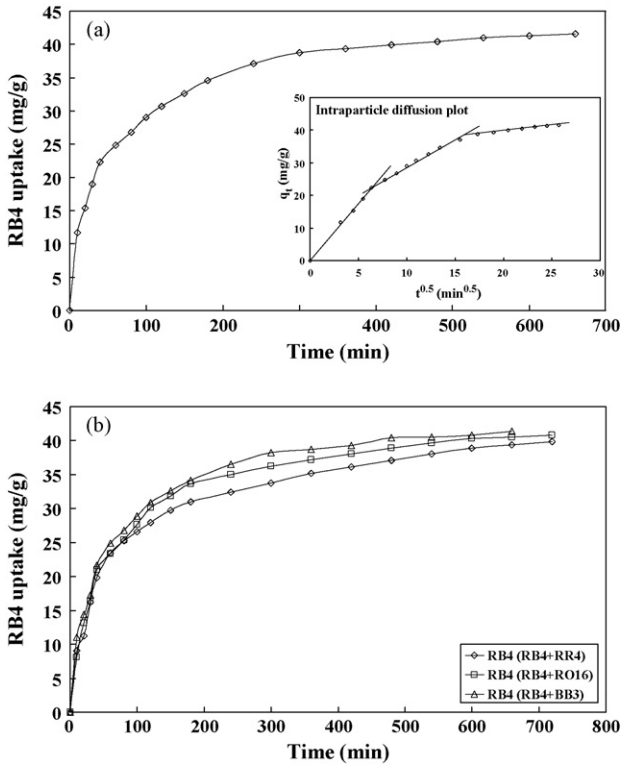

Fig. 4. Biosorption kinetics of single (a) and binary (b) dye systems [pH 3; temperature = 25 °C; agitation speed = 160 rpm; C_0 (single-dye) = 248 mg/L; C_0 (multi-dye) = 498 ± 2 mg/L]. Intraparticle diffusion plot (a) showing multiple slopes.

which is based on the assumption that there is an exponential distribution of adsorption energies available for each solute. Interestingly, the model was able to describe all three binary isotherms, with relatively high correlation coefficients and low % error values, within the ranges of 0.62–0.99 and 1.6–21.6%, respectively. As already proved in our experiments, that the magnitude of RB4 competition over other dyes was significant, and this data got confirmed by the SRS equation yielding high competitive coefficients of 0.71, 1.52 and 0.21 during RB4–RR4, RB4–RO16 and RB4–BB3 biosorption.

3.4. Biosorption kinetics

Shown in Fig. 4a is the plot of RB4 uptake onto PIPC against time. Since the biomass was immobilized, the rate of dye uptake was slow and final equilibrium was reached only around 300 min. For immobilization systems, the biomass was retained in the interior of immobilized matrix and mass transfer resistances play a significant role in deciding the rate of biosorption. However, for successful immobilization systems these mass transfer resistances should not influence the overall biosorption performance of biomass. Most importantly, the dye molecules should have access to all possible binding sites even at a slower rate. In an attempt to visualize the influence of mass transfer resistance on dye uptake, the kinetic data were analyzed using the equation as proposed by Weber and Morris [26]:

$$q_t = k_i t^{1/2} \quad (12)$$

According to the Weber–Morris model, the plot of q_t versus $t^{1/2}$ should be linear if intraparticle diffusion is involved in the sorption process, and if this line passes through the origin, then intraparticle diffusion is the rate controlling step. Various steps of dye transfer from bulk solution to binding sites have been reported in the literature [27,28]. The first step, viz. sorption of RB4 over the surface of biomass is usually fast because of proper mixing. The second step involves diffusion of dye through a hydrodynamic boundary layer around the biosorbent surface (intraparticle diffusion). The third step, viz. sorption of dye by the biomass binding sites [29]. From RB4 kinetic data, the influence of intraparticle diffusion (Fig. 4a) can be clearly seen; however, it cannot be assumed as the fully operative mechanism, since the slope of the second portion is not passing through the origin. The calculated value of intraparticle diffusion constant (k_i) was 1.54 mg/(g $min^{0.5}$).

In the case of binary dye systems, the rate of dye uptake depends not only on the diffusion mechanisms, but also on the extent of competition between dye solutes. Each reactive dye will repel the other, and compete to occupy the same binding sites. These factors usually delay the equilibrium attainment; which was also observed in our experiments (Fig. 4b). Therefore, it is not appropriate to describe the multicomponent kinetics data using the Weber–Morris model and; thus, was not attempted in this study.

3.5. Reuse of biosorbent

To investigate the feasibility of reusing PIPC beads in multiple cycles, batch desorption experiments were conducted. Biosorption experiments revealed that RB4 could be effectively sorbed under acidic conditions and; therefore, desorption would be expected under alkaline conditions. Considering this, 0.1 M NaOH was used as an elutant and its performance was very satisfactory as elution efficiency of 99% was obtained. Under strong basic (high pH) conditions, the number of negatively charged sites increases. These negatively charged sites on the sorbent surface favor desorption of dye anions due to electrostatic repulsion.

Next, experiments were conducted to reuse the PIPC beads for RB4 biosorption for 10 cycles. PIPC beads approximately retained their first cycle RB4 uptake throughout the 10 cycles examined, aided with consistently high elution efficiencies around 99% by 0.1 M NaOH. Most importantly, the weight loss was insignificant (<2.1%) at the end of tenth cycle. The constant RB4 uptake capacity of polysulfone immobilized *C. glutamicum* is very interesting, since the binding sites were active enough to accommodate RB4 during multiple cycles and the stability of polysulfone matrix in the entrapment of biomass. The RB4 biosorption capacities and removal efficiencies were always greater than 40.7 mg/g and 91.2%, respectively, during regeneration cycles. The decrease in RB4 biosorption capacity was insignificant as only 3.3% was observed at the end of tenth cycle.

3.6. Biosorption column experiments

In process applications, a packed bed column is an effective arrangement for cyclic sorption/desorption, as it makes the

Table 2
Sorption process parameters during single and binary dye biosorption using PIPC

Type of dye solution	Uptake (mg/g)	Breakthrough time (h)	Exhaustion time (h)	dc/dt[a] (mg/(L h))	Dye removal (%)
RB4	92.9	12.8	64.2	2.1	63.9
RB4 + RR4					
RB4	77.8	7.1	63.1	1.9	56.3
RR4	42.8	1.8	37.1	2.8	42.7
RB4 + RO16					
RB4	82.9	7.8	59.4	2.0	60.3
RO16	56.7	2.3	40.2	2.9	62.1
RB4 + BB3					
RB4	85.9	12.1	65.9	2.1	59.3
BB3	7.8	ud	9.8	ud	31.2

ud, undetectable.
[a] Slope of the breakthrough curve from breakthrough to exhaustion time.

best use of the concentration difference known to be a driving force for biosorption and results in a better quality of the effluent [30,31]. In the first series of the column experiments, the PIPC-loaded column was exposed to pure RB4 solution. Initially, the column was packed with 4.8 g (wet weight)/1.1 g (dry weight) PIPC, yielding an initial bed height and volume of 10 cm and 7.85 mL, respectively. The breakthrough curve is shown in Fig. 5, with the column parameters listed in Table 2. The definition and evaluation of column parameters was based on our previous study [5,32]. The PIPC bed allowed RB4 breakthrough to occur at 12.8 h and complete exhaustion at 64.2 h.

Next, the interference of RR4, RO16 and BB3 during RB4 biosorption was studied (Fig. 5). In all cases of binary systems, the competing dyes tend to overshoot earlier than RB4, thereby considerably reducing the service time of the column. Also, the background of competing dyes had a significant effect on the binding of target dye. Among the competitive dyes, RR4 severely affected the RB4 breakthrough time, uptake and % removal; followed by RO16 and BB3 (Table 2). The decrease in RB4 uptake, compared to pure RB4 system, was in the order of 19.5, 12.2 and 8.1% in the presence of RR4, RO16 and BB3, respectively. On comparing RO16 and RR4 biosorption in the presence of RB4, the performance of PIPC onto RO16 was superior. A delayed RO16 breakthrough with high uptake and % removal were observed. This clearly indicates that the stoichiometric relationship between sulfonate groups of reactive dyes and amine groups of biomass played a major role in column biosorption. In contrary to reactive dyes, BB3 is unable to compete with RB4 biosorption as almost similar RB4 breakthrough curves were observed in the presence or absence of BB3 (Fig. 5). Also, PIPC exhibited inferior BB3 biosorption at the column operating condition of pH 3; as undetectable column breakthrough ($t_b < 0.5$ h) and very earlier exhaustion ($t_e = 9.8$ h) were obtained.

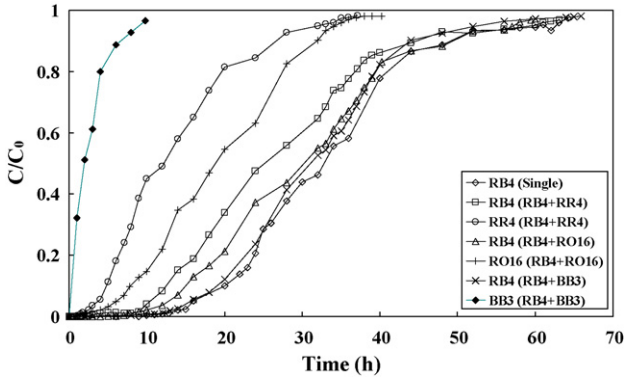

Fig. 5. Breakthrough curves during single and binary dye biosorption in the up-flow PIPC loaded column [bed height = 10 cm; flow rate = 0.5 mL/min; inlet solution pH 3; C_0 (single-dye) = 100 mg/L; C_0 (multi-dye) = 199 ± 1 mg/L].

In the final stage of column experiments, the PIPC column loaded with pure RB4 was eluted using 0.1 M NaOH. The elution curve (figure not shown) exhibited a general trend; that is, a sharp increase at the beginning, followed by a gradual decrease. The elution process was carried out for 4.6 h with elution efficiency of 98.4%. The concentration factor [33] which can be used to assess the overall achievement of the biosorption process, can be defined as the ratio of volume of effluent treated (in sorption process) to the volume of elutant used (in desorption process). The concentration factor was determined as 7; and this implies high concentrated dye in small volume of elutant.

4. Conclusions

Industrial effluents emanating from textile-based industries often comprise of several dye components. Hence the dye remediation methods should take the interaction and competition among the dye components into consideration, before designing the treatment process. The affinity of a dye towards a particular sorbent may be due to various reasons, which usually depends on the property of the dye itself. For instance, in this study, the competition incurred by RR4, RO16 and BB3 during biosorption of RB4 onto PIPC was studied. During which, we found that PIPC showed high preference towards RB4, when the dye was present in its pure form; while the presence of RR4 and RO16 diminished the RB4 uptake. Molecular weight, number of sulfonate groups and reactivity of each reactive dye played a vital role in deciding the order of preference towards the amine groups of PIPC; and it can be generalized on the molar uptake as RB4 > RO16 > RR4.

With the limited availability of active amine groups and repulsion caused by each dye anions in binary dye mixtures, the single system dye uptake was higher than that of multi-dye systems. Utilization of up-flow packed column to study the competition between dyes produced interesting results, which include earlier breakthrough of competing dyes (RR4, RO16 and BB3) compared to dye of interest (RB4) and decreased RB4 column performance because of competing dyes. In summary, this study has emphasized the importance of detailed investigations on the competition and interaction between dyes, which are more likely to occur in reality.

Acknowledgements

This work was supported by a grant from the Post-Doc program, Chonbuk National University (the second half term of 2006) and, in part, by KOSEF through AEBRC at POSTECH.

References

[1] P.R. Puranik, K.M. Paknikar, Biosorption of lead and zinc from solutions using *Streptoverticillium cinnamoneum* waste biomass, J. Biotechnol. 55 (1997) 113–124.
[2] S.W. Won, S.B. Choi, B.W. Chung, D. Park, J.M. Park, Y.-S. Yun, Biosorptive decolorization of Reactive orange 16 using the waste biomass of *Corynebacterium glutamicum*, Ind. Eng. Chem. Res. 43 (2004) 7865–7869.
[3] T. Hermann, Industrial production of amino acids by coryneform bacteria, J. Biotechnol. 104 (2003) 155–172.
[4] S.W. Won, S.B. Choi, Y.-S. Yun, Interaction between protonated waste biomass of *Corynebacterium glutamicum* and anionic dye Reactive red 4, Colloids Surf. A: Physicochem. Eng. Aspects 262 (2005) 175–180.
[5] K. Vijayaraghavan, Y.-S. Yun, Chemical modification and immobilization of *Corynebacterium glutamicum* for biosorption of Reactive black 5 from aqueous solution, Ind. Eng. Chem. Res. 46 (2007) 608–617.
[6] K. Vijayaraghavan, Y.-S. Yun, Utilization of fermentation waste (*Corynebacterium glutamicum*) for biosorption of Reactive black 5 from aqueous solution, J. Hazard. Mater. 141 (2007) 45–52.
[7] F. Vegliò, F. Beolchini, Removal of metals by biosorption: a review, Hydrometallurgy 44 (1997) 301–316.
[8] R.S. Bai, T.E. Abraham, Studies on chromium(VI) adsorption–desorption using immobilized fungal biomass, Bioresour. Technol. 87 (2003) 17–26.
[9] E.N. El Qada, S.J. Allen, G.M. Walker, Adsorption of basic dyes onto activated carbon using microcolumns, Ind. Eng. Chem. Res. 45 (2006) 6044–6049.
[10] K.K.H. Choy, J.F. Porter, G. McKay, Langmuir isotherm models applied to the multicomponent sorption of acid dyes from effluent onto activated carbon, J. Chem. Eng. Data 45 (2000) 575–585.
[11] M.-S. Chiou, G.-S. Chuang, Competitive adsorption of dye metanil yellow and RB15 in acid solutions on chemically cross-linked chitosan beads, Chemosphere 62 (2006) 731–740.
[12] B. Al-Duri, G. McKay, Prediction of binary systems of batch adsorption using basic dyes onto activated carbon, Chem. Eng. Sci. 46 (1991) 193–204.
[13] G. McKay, B. Al-Duri, Simplified model for the equilibrium adsorption of dyes from mixtures using activated carbon, Chem. Eng. Process 22 (1987) 145–156.
[14] C. Sheindrof, M. Rebhun, M. Sheintuch, A Freundlich type multicomponent isotherm, J. Colloids Interf. Sci. 79 (1981) 136–142.
[15] V.P. Vinod, T.S. Anirudhan, Adsorption behavior of basic dyes on the humic acid immobilized pillared clay, Water Air Soil Pollut. 150 (2003) 193–217.
[16] Y.-S. Yun, D. Park, J.M. Park, B. Volesky, Biosorption of trivalent chromium on the brown seaweed biomass, Environ. Sci. Technol. 35 (2001) 4353–4358.
[17] P. Lodeiro, B. Cordero, Z. Grille, R. Herrero, M.E.S. de Vicente, Physicochemical studies of cadmium(II) biosorption by the invasive alga in Europe *Sargassum muticum*, Biotechnol. Bioeng. 88 (2004) 237–247.
[18] M.E. Romero-Gonzalez, C.J. Williams, P.H.E. Gardiner, Study of the mechanisms of cadmium biosorption by dealginated seaweed waste, Environ. Sci. Technol. 35 (2001) 3025–3030.
[19] L. Eggeling, H. Sahm, The cell wall barrier of *Corynebacterium glutamicum* and amino acid efflux, J. Biosci. Bioeng. 92 (2001) 201–213.
[20] P. Hünten, N. Costa-Riu, D. Palm, F. Lottspeich, R. Benz, Identification and characterization of PorH, a new cell wall channel of *Corynebacterium glutamicum*, Biochim. Biophys. Acta 1715 (2005) 25–36.
[21] H. Mètivier-Pignon, C. Faur-Brasquet, P. Le Cloirec, Adsorption of dyes onto activated carbon cloths: approach of adsorption mechanisms and coupling of ACC with ultrafiltration to treat coloured wastewaters, Sep. Purif. Technol. 31 (2003) 3–11.
[22] C. Faur, H. Mètivier-Pignon, P. Le Cloirec, Multicomponent adsorption of pesticides onto activated carbon fibers, Adsorption 11 (2005) 479–490.
[23] A. Kawabata, J.A. Taylor, The effect of reactive dyes upon the uptake and anti bacterial action of poly(hexamethylene biguanide) on cotton. Part 2. Uptake of poly(hexamethylene biguanide) on cotton dyed with β-sulphatoethylsulphonyl reactive dyes, Dyes Pigments 68 (2006) 197–204.
[24] R.-S. Juang, H.-J. Shao, Effect of pH on competitive adsorption of Cu(II), Ni(II) and Zn(II) from water onto chitosan beads, Adsorption 8 (2002) 71–78.
[25] J.A. Fowler, W.J. Marshall, Reactive dyes: the technical basis for choosing between dyes of high and dyes of low reactivity, J. Soc. Dyers Colourists 80 (1964) 358–363.
[26] W.J. Weber, J.C. Morris, Kinetics of adsorption on carbon solution, J. Sanit. Eng. Div. Am. Soc. Civil Eng. 89 (1963) 31–60.
[27] S.J. Allen, Q. Gan, R. Matthews, P.A. Johnson, Mass transfer processes in the adsorption of basic dyes by peanut hulls, Ind. Eng. Chem. Res. 44 (2005) 1942–1949.
[28] A. Özcan, E.M. Öncü, A.S. Özcan, Kinetics, isotherm and thermodynamic studies of adsorption of acid blue 193 from aqueous solutions onto natural sepiolite, Colloids Surf. A: Physicochem. Eng. Aspects 277 (2006) 90–97.
[29] B. Guo, L. Hong, H.X. Jiang, Macroporous poly(calcium acrylate-divinylbenzene) bead—a selective orthophosphate sorbent, Ind. Eng. Chem. Res. 42 (2003) 5559–5567.
[30] Y. Fu, T. Viraraghavan, Column studies for biosorption of dyes from aqueous solutions on immobilized *Aspergillus niger* fungal biomass, Water SA 29 (2003) 465–472.
[31] Z. Aksu, Ş.Ş. Çağatay, F. Gönen, Continuous fixed bed biosorption of reactive dyes by dried *Rhizopus arrhizus*: determination of column capacity, J. Hazard. Mater. 143 (2007) 362–371.
[32] K. Vijayaraghavan, J. Jegan, K. Palanivelu, M. Velan, Batch and column removal of copper from aqueous solution using a brown marine alga *Turbinaria ornata*, Chem. Eng. J. 106 (2005) 177–184.
[33] K. Vijayaraghavan, K. Palanivelu, M. Velan, Crab shell-based biosorption technology for the treatment of nickel-bearing electroplating industrial effluents, J. Hazard. Mater. B119 (2005) 251–254.